

Galaxy groups in the 2dF redshift survey: The catalogue

Manuel Merchán & Ariel Zandivarez

*Grupo de Investigaciones en Astronomía Teórica y Experimental, IATE, Observatorio Astronómico, Laprida 854, Córdoba, Argentina
Consejo de Investigaciones Científicas y Técnicas de la República Argentina*

1 February 2008

ABSTRACT

We construct a galaxy groups catalogue from the public 100K data release of the 2dF galaxy redshift survey. The group identification is carried out using a slightly modified version of the group finding algorithm developed by Huchra & Geller. Several tests using mock catalogues allow us to find the optimal conditions to increase the reliability of the final group sample. A minimum number of 4 members, an outer number density enhancement of 80 and a linking radial cutoff of 200 km sec^{-1} , are the best obtained values from the analysis. Using these parameters, approximately 90% of groups identified in real space have a redshift space counterpart. On the other hand the level of contamination in redshift space reaches to 30 % including a $\sim 6\%$ of artificial groups and $\sim 24\%$ of groups associated with binaries or triplets in real space. The final sample comprise 2209 galaxy groups covering the sky region described by Colless et al. spanning over the redshift range of $0.003 \leq z \leq 0.25$ with a mean redshift of 0.1.

Key words: galaxies: groups - finding algorithms - mock catalogues

1 INTRODUCTION

The study of galaxy groups is a very interesting area of research because these density fluctuations lay between galaxies and clusters of galaxies and may provide important clues to galaxy formation.

Since the appearing of large galaxy redshift surveys more reliable detection of group of galaxies have been possible. Two pioneer works develop the main identification algorithms. The first was introduced by Huchra & Geller (1992) and the second was proposed by Nolthenius & White (1987); both are friends-of-friends algorithms, differing only in the scaling of the linking lengths. Frederic (1995) perform an extensive study of these algorithms using N-body simulations, concluding that neither of them is intrinsically superior to the other, and the choice of one of them depends on the purpose for which groups are to be studied. Recently several catalogues have been constructed from different large galaxy redshift surveys using these algorithms. Merchán et al. (2000) use the Updated Zwicky Catalogue (Falco et al. 1999) generating a sample of 517 galaxy groups. Using the Nearby Optical Galaxy Sample, Giuricin et al. (2000) construct one of the large catalogue of loose groups and Tucker et al. (2000) found 1495 groups in the Las Campanas Redshift Survey. Finally, Ramella et al. (2002) generate a group catalogue of 1168 members from the combination of the Updated Zwicky Catalogue and the Southern Sky Redshift Survey (da Costa et al. 1998).

At the present, the largest sample of galaxies with spec-

troscopic redshifts (~ 100000) is the Anglo-Australian two degree field galaxy redshift survey (hereafter 2dFGRS, Colless et al. 2001). The survey covers 2000 deg^2 and has a median depth $\bar{z} = 0.11$.

Several studies were done with this preliminary sample by the 2dFGRS Team. Some of them are the power spectrum of galaxies (Percival et al. 2001), the projected two point correlation function of galaxies for different volume limited samples (Norberg et al. 2001a), and the estimation of the b_J band galaxy luminosity function (Norberg et al. 2001b). Another study related with system of galaxies in the 2dFGRS has been carried out by De Propriis et al. (2002) where they present an study of 3-dimensional galaxy clusters based on well known bidimensional galaxy clusters.

The large number of galaxies and the depth of the 2dFGRS make it very suitable for galaxy groups identification. Nevertheless the present release of the sample is not uniform due to variations in sky coverage which make difficult the analysis of the data.

The main objective of this work is the identification of groups in the 2dFGRS and estimation of their physical properties (number of members, velocity dispersion, virial radius and mass). In order to take into account the variation in the sky coverage of the 2dFGRS we introduce a couple of modifications to the group-finding algorithm developed by Huchra & Geller (1982). The first one deals with the apparent magnitude limit variation across the sky and the second is related to redshift completeness. These modifications are tested using mock catalogues which reproduce

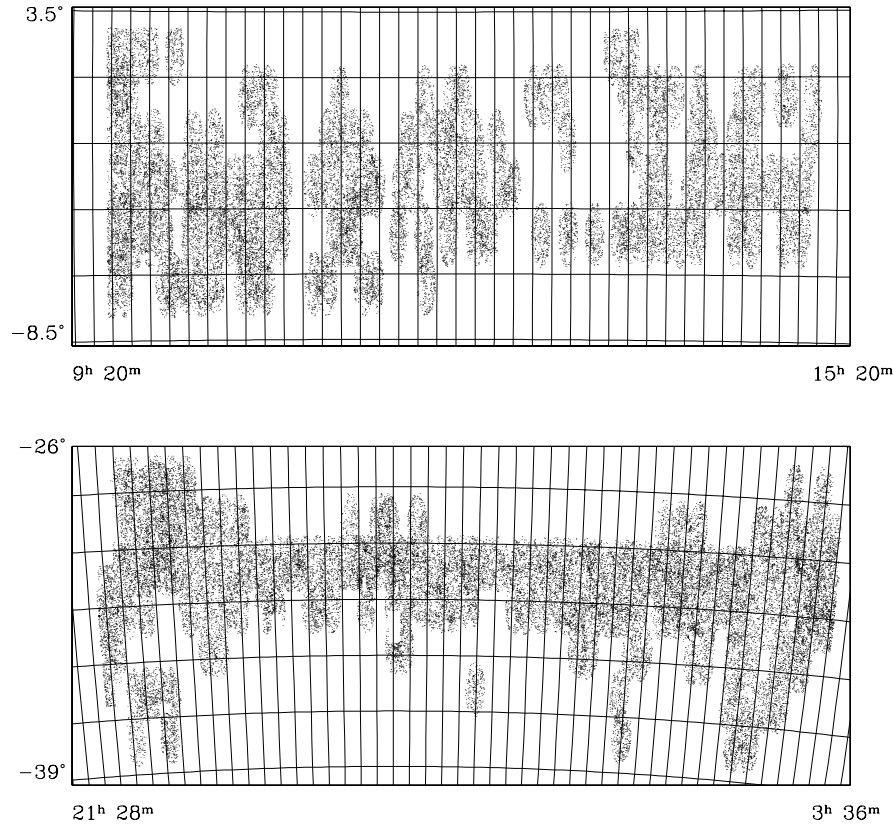


Figure 1. Aitoff projections of the 2dFGRS. The upper projection represent the distribution of galaxies in equatorial coordinates in the northern strip and the lower the southern one.

each effect separately. We also use these mock catalogues to explore the space of linking parameters to maximize group identification accuracy.

The paper is structured as follows. The catalogue is described in section 2. In section 3 we describe the group finder algorithm used to identify galaxy groups in the 2dFGRS. A detailed test of the method is performed in section 4. Finally, the 2df group catalogue is presented in section 5 followed by conclusions in section 6.

2 THE GALAXY CATALOGUE

The complete 2dFGRS will consist of approximately 250000 galaxies with redshifts in two declination strips plus 100 random 2-degree fields. All targets are selected in the photometric b_j band from the APM galaxy survey (Maddox et al. 1990a,b;1996). The southern strip (SGP) covers approximately 1275 square degrees ($-37^\circ.5 \leq \delta \leq -22^\circ.5$; $21^h 40^m \leq \alpha \leq 3^h 30^m$) and the northern strip (NGP) covers 750 square degrees ($-7^\circ.5 \leq \delta \leq 2^\circ.5$; $9^h 50^m \leq \alpha \leq 14^h 50^m$) while the 100 random fields are spread uniformly over the 7000 square degrees in the southern region.

In our analysis we use the 2dF public 100K data release of galaxies with the best redshift estimates within the two main strips (NGP and SGP) of the catalogue. Given the

status of the project, the sky coverage of the sample is not uniform, so a detailed completeness description is needed (see Figure 1). For this purpose, we use in our analysis the 2dFGRS mask software constructed by Peder Norberg and Shaun Cole which take into account both the magnitude limit and the redshift completeness (see also Figure 13 and 15 of Colless et al. 2001). The redshift completeness was defined with the 2° field used to tile the survey region for spectroscopic observations. This quantity is the ratio of the number of galaxies for which redshifts have been obtained to the total number of objects contained in the parent catalogue and has a mean value of ~ 0.75 for the whole sample. On the other hand, the magnitude limit mask corresponds to variations of the parent survey magnitude limit with the position on the sky. This variation span over a magnitude limit range of $m = 18.95 - 19.55$ for the NGP and a range of $m = 19.3 - 19.55$ for the SGP. This sample comprise 102426 galaxies with final b_j magnitudes corrected for galactic extinction.

3 THE GROUP-FINDING ALGORITHM

For group identification we use a friends-of-friends algorithm similar to that described by Huchra & Geller (1982) modi-

fied in order to take into account redshift completeness and magnitude limit variations.

If we have a pair of galaxies with mean radial velocity $V = (V_1 + V_2)/2$ and angular separation θ_{12} , our algorithm links galaxies when the following conditions are satisfied:

$$D_{12} = 2 \sin\left(\frac{\theta_{12}}{2}\right) \frac{V}{H_0} \leq D_L \quad (1)$$

and

$$V_{12} = |V_1 - V_2| \leq V_L \quad (2)$$

where D_{12} is the angular separation and V_{12} is the line-of-sight velocity difference. The transverse D_L and radial linking lengths V_L are scaled as $D_0 R$ and $V_0 R$ respectively in order to compensate for the decline of the selection function with distance. The scaled factor is computed as

$$R = \left[\frac{\int_{-\infty}^{M_{12}} \phi(M) dM}{\int_{-\infty}^{M_{lim}} \phi(M) dM} \right]^{-1/3} \quad (3)$$

where M_{lim} and M_{12} are the absolute magnitude of the brightest galaxy visible at a distance V_f/H_0 and V/H_0 respectively. In these equations, D_0 and V_0 are the linking cutoffs at the fiducial velocity V_f , and $\phi(M)$ is the galaxy luminosity function of the sample.

In the special case of the 2dFGRS, we should take into account the magnitude limit and completeness variations through the sky. The adopted way to solve this issue consists in defining an average magnitude limit for each pair

$$m_{lim} = (m_{lim}^1 + m_{lim}^2)/2 \quad (4)$$

and redefining the scale factor R as

$$R = \left[\frac{\int_{-\infty}^{M_{12}} \phi(M) dM}{\int_{-\infty}^{M_{lim}} \phi(M) dM} \frac{(C_1 + C_2)}{2} \right]^{-1/3} \quad (5)$$

where C_1 and C_2 are the corresponding completeness values for each galaxy position on the sky.

4 TESTING THE METHOD

4.1 Mock Catalogues

To examine the degree of accuracy of our algorithm we use a set of mock catalogues constructed from a gravitational numerical simulation of a flat low density cold dark matter universe. We perform this simulation using the Hydra Nbody code developed by Couchman et. al (1995) with 128^3 particles in a cubic comoving volume of $180 h^{-1}$ Mpc per side starting at $z=50$. The adopted cosmological model was a universe with $\Omega_m = 0.3$, $\Omega_\Lambda = 0.7$, Hubble constant $h = 0.7$ and a relative mass fluctuation of $\sigma_8 = 0.9$.

In order to reproduce the same radial distribution as in the 2dFGRS, we adopt a galaxy luminosity function fitted by a Schechter function with $M_{b_j}^* - 5 \log_{10} h = -19.66$, $\alpha = -1.21$, $\Phi^* = 1.68 \times 10^{-2} h^3 \text{Mpc}^{-3}$ and a model of the average k+e correction given by the formula

$$k(z) + e(z) = \frac{z + 6z^2}{1 + 20z^3} \quad (6)$$

(see Norberg et al. 2001b). Combining these models and

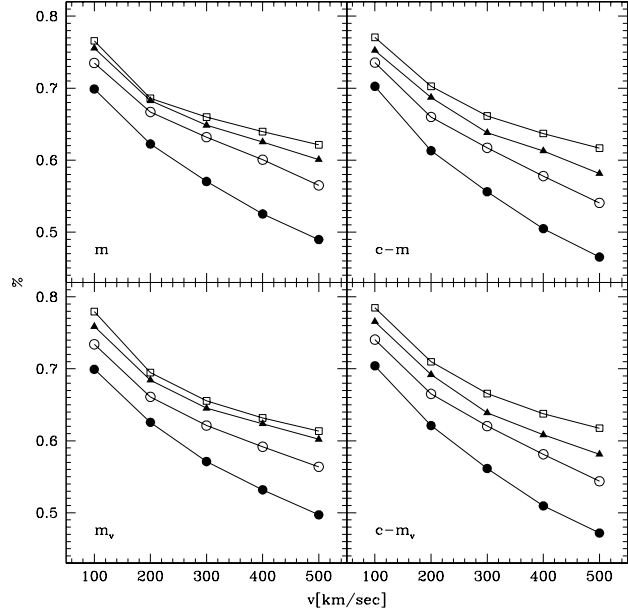


Figure 2. The percentage of groups found in redshift space which match with some group in real space. These percentage are shown spanning the parameter space V_0 (100, 200, 300, 400 and 500 km^{-1}) $\delta\rho/\rho$ (20-filled circles, 40-open circles, 80-filled triangles and 160-open squares). Each panel show the different kind of mocks constructed.

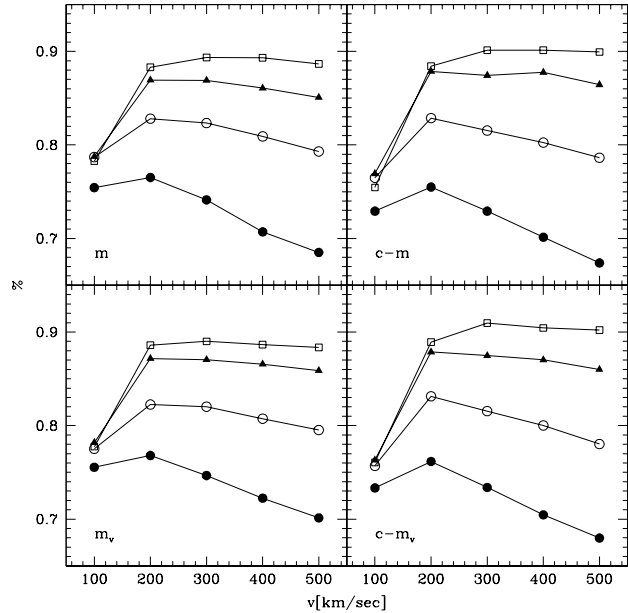


Figure 3. The percentage of the group catalogue in real space associated with the catalogue of matched groups in redshift space. The symbols and the panels are the same as in Figure 2.

using the positions from the simulation we generate an apparent magnitude

$$m = k + e + 5 \log_{10}(d_L/h^{-1} \text{Mpc}) + 25 + (M_{b_j} - 5 \log_{10} h)(7)$$

for each particle inside the angular mask described in section 2. We construct four mock catalogues with different sky coverage:

- in the first mock we introduce a fixed faint survey magnitude limit (m);
- the second mock has a fixed faint survey magnitude limit and the effect of redshift completeness as in the real survey ($c - m$);
- the third mock has a faint survey magnitude limit which changes with the angular position of a particle in the same way as the magnitude limit mask of the 2dFGRS (m_v);
- finally, the fourth mock have both effects, the magnitude limit mask and the redshift completeness mask ($c - m_v$).

4.2 Identification Accuracy

From the mock catalogues described in the previous section, we identify groups in real and redshift spaces. The former identification is carried out using the same linking length in both directions ($V_0 = D_0$) whereas different linking lengths are used in redshift space. The fiducial velocity V_f is adopted as 1000 km s^{-1} in all identifications. The linking lengths are selected spanning the space parameter ($V_0, \delta\rho/\rho$) where the later is the number density contour surrounding a group and corresponds to a fixed number density enhancement relative to the mean number density of

$$\frac{\delta\rho}{\rho} = \frac{3}{4\pi D_0^3} \left(\int_{-\infty}^{M_{lim}} \Phi(M) dM \right)^{-1} - 1 \quad (8)$$

The selected values are:

- V_0 : 100, 200, 300, 400 and 500 km s^{-1}
- $\delta\rho/\rho$: 20, 40, 80 and 160

To quantify how good are the groups identified in redshift space we implement a method to match the center of mass of these groups with the center of mass of groups in real space. Our method seeks for groups in real space within a projected and a radial distance having its origin in the center of mass of each group in redshift space. We choose the searching parameters in order to maximize the matching, nevertheless the results are very stable around the chosen values. The results show that almost all groups have one match inside the limits and only a few are related with two or three groups in real space. In the later situation we choose to associate the group in redshift space with that group in real space with more shared particles.

The first result from this comparison is that the percentage of spurious groups identified is remarkably higher when we include groups in redshift space with 3 members ($\sim 40\%$). Ramella, Geller & Huchra (1989) and Frederic (1995) obtain that one-third or more of the groups identified in redshift space with $N=3$ are spurious, which is roughly consistent with our result. Consequently, we adopt as the main catalogue all groups identified in redshift space with more than 4 members. Figure 2 shows the number of groups which match with one group in real space relative to the

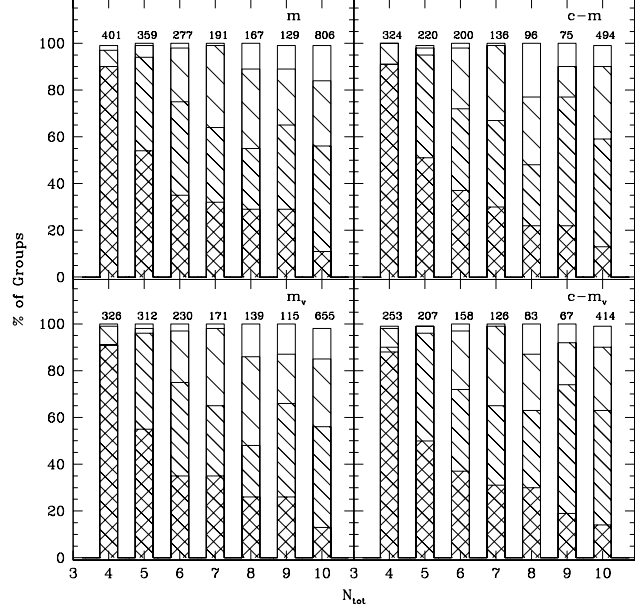


Figure 4. Fraction of groups of a given richness N_{tot} with \mathcal{F} . Cross hatched regions show a ratio \mathcal{F} of unity, single narrow hatched regions correspond to $0.75 \leq \mathcal{F} < 1$, $0.5 \leq \mathcal{F} < 0.75$ to single wide hatched regions and no hatching regions belong to $0.25 \leq \mathcal{F} < 0.5$. For richness 10 we include all groups with 10 or more members. The labels over the bars show the number of groups for the corresponding richness.

total number of groups in the main catalogue. The analysis comprises all mock and identification parameters under consideration. The complementary percentage in each case represents the spurious groups in the main catalogue. We consider spurious those groups which do not have any match or are associated with a binary or a triplet in real space. The individual percentages for these spurious groups for the $c - m_v$ mock are shown in Table 1 where the first line represents no matched groups, the second and third lines correspond to binaries and triplets respectively.

We also analyse the percentage of the group catalogue in real space associated with matched groups in the main catalogue. That percentage is plotted in Figure 3 for all the options as in Figure 2. Despite the percentage of matched groups in the main catalogue seems to be the highest for a velocity of 100 km s^{-1} and density contrast of 160, it can be seen from Figure 3 that this choice represents one of the lowest percentages of the group catalogue in real space. Combining the two figures we can conclude that the best options are a velocity of 200 km s^{-1} and density contrast of 80 or 160. We choose a density contrast of 80 because the total number of groups identified is greater and the matching accuracy is roughly similar.

The resulting value of $\delta\rho/\rho = 80$ is in agreement with that obtained by Ramella et al. (1997) for the CfA2 Redshift Survey, whereas our optimal velocity linking parameter $V_0 = 200 \text{ km s}^{-1}$ differs from his choice ($V_0 = 350 \text{ km s}^{-1}$). Should be taken into account that equal $\delta\rho/\rho$ correspond to different values of D_0 depending of the apparent magnitude limit of the survey. Particularly, the the apparent magnitude

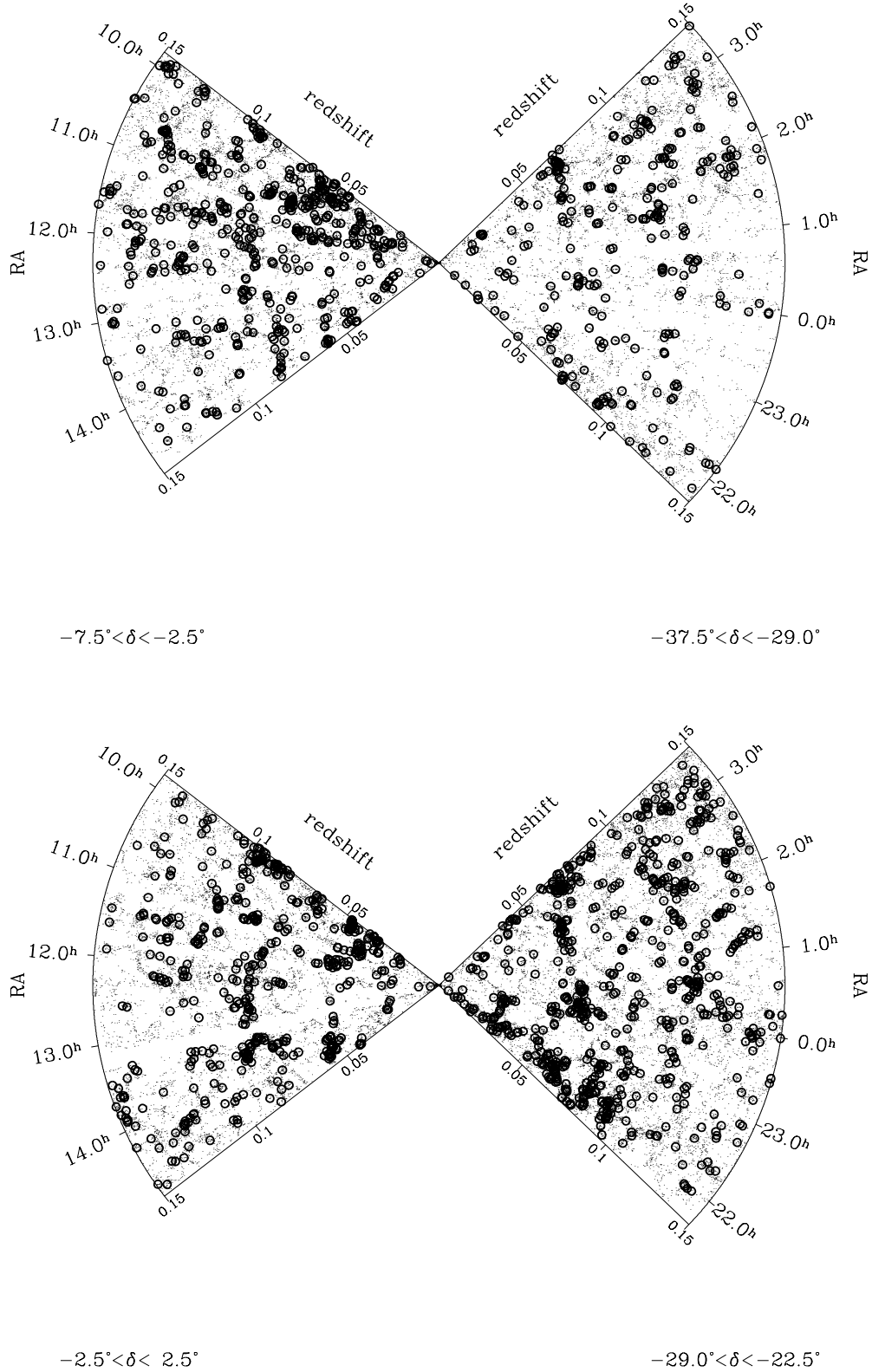
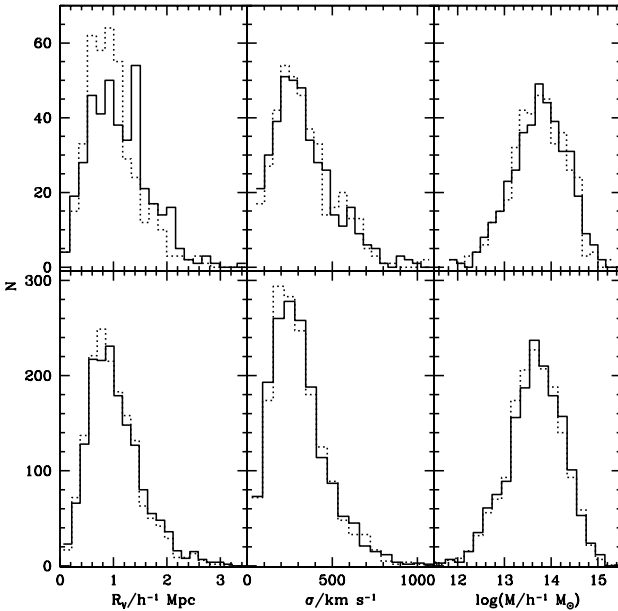


Figure 5. The redshift distribution for the galaxy groups identified in the 2dFGRS. The pieplot show at the left the NGP of the 2dFGRS and the SGP at right. The dots are the galaxies and the open circles the galaxy groups. To make the plot clearer we limit the plot to $z < 0.15$

Table 1. Percentage of spurious groups identified in the $c - m_v$ mock

V_0 (km s^{-1})	$\delta\rho/\rho$			
	20	40	80	160
100	13	9	6	4
	7	8	8	8
	9	9	9	9
200	16	10	6	5
	10	10	11	10
	12	13	13	14
300	19	12	9	6
	11	12	13	12
	13	14	14	15
400	23	14	10	7
	13	13	14	14
	13	15	15	15
500	26	17	12	8
	14	14	15	14
	14	15	15	16

**Figure 6.** Upper and lower panels show the distribution of the main physical properties of groups at low and high completeness regions respectively. Solid and dotted lines correspond to groups with and without border effects.

limits for the 2dFGRS and the CfA2 Redshift Survey are ~ 19.4 and 15.5 respectively. Consequently, the higher number density of the 2dFGRS implies smaller linking parameters than those obtained for the CfA2 Redshift Survey.

From the comparison between the four kind of mock catalogues we conclude that implemented modifications keep the behavior of the original algorithm, showing the ability of

these modifications to deal with an inhomogeneous galaxy samples like the 2dFGRS.

To examine the degree of agreement between members of groups in real and redshift space we perform an analysis similar to Frederic (1995) for matched groups in the main catalogue. If we define the total number of members of a given group in redshift space as N_{tot} , we search how many members of this group are in the associated group in real space N_m and compute the ratio $\mathcal{F} = N_m/N_{tot}$. Figure 4 shows the fraction of groups of a given richness N_{tot} with \mathcal{F} for several values: 1 (cross hatched regions), $0.75 \leq \mathcal{F} < 1$ (single narrow hatched regions), $0.5 \leq \mathcal{F} < 0.75$ (single wide hatched regions) and $0.25 \leq \mathcal{F} < 0.5$ (no hatching regions). For richness 10 we include all groups with 10 or more members. As it can be seen, more than $\sim 65\%$ of the groups have a ratio \mathcal{F} greater than 0.75 for all kind of mocks. It also should be noticed that the implemented modifications keep the performance of the original Huchra & Geller algorithm.

We still need to test that our modifications to the Huchra & Geller algorithm improve the detection of galaxy groups. In order to prove the modification which take into account the redshift completeness we compare the results of the identification using both, modified and original Huchra & Geller algorithms on the $c - m$ mock catalogue. As result, we find that the identification using our modification produce 263 ($\sim 11\%$ of the total sample) more groups than the corresponding to the plain algorithm version. On the other hand, the wide apparent magnitude limit range implies a variation in the local number density, which produce a similar effects as the redshift completeness. This effect was tested applying a similar procedure as the former but using the m_v mock catalogue. The results show a difference of 89 groups using our modified algorithm against the original Huchra & Geller one. The effect due to the apparent magnitude limit is smaller than the observed for the redshift completeness because the magnitude limit distribution have a mean value of ~ 19.4 tending to the upper limit of the whole range. Finally, we test the joint effects applying the same procedure to the $c - m_v$ mock catalogue, showing that our modification identify 280 more groups ($\sim 14\%$ of the total sample). As we have shown in the previous tests, the modified algorithm keep the performance of the original Huchra & Geller method, then the $\sim 70\%$ of these differences correspond to real groups for the chosen linking parameters.

5 GALAXY GROUP IDENTIFICATION IN THE 2DFGRS

To identify groups in the 2dF survey (2dFGGC), we adopt the values $\delta\rho/\rho = 80$ and $V_0 = 200 \text{ km s}^{-1}$ which maximize the group accuracy as shown in section 4.

The resulting groups catalogue contains systems with at least 4 members, mean radial velocities in the range $900 \text{ km s}^{-1} \leq V \leq 75000 \text{ km s}^{-1}$ and a total number of 2209 groups. It represents the largest sample to the present and provides a suitable data set to analyse the clustering properties of galaxy systems of low richness. As discussed in the previous section, the limit adopted in the number of members in galaxy groups is necessary in order to avoid pseudo-groups.

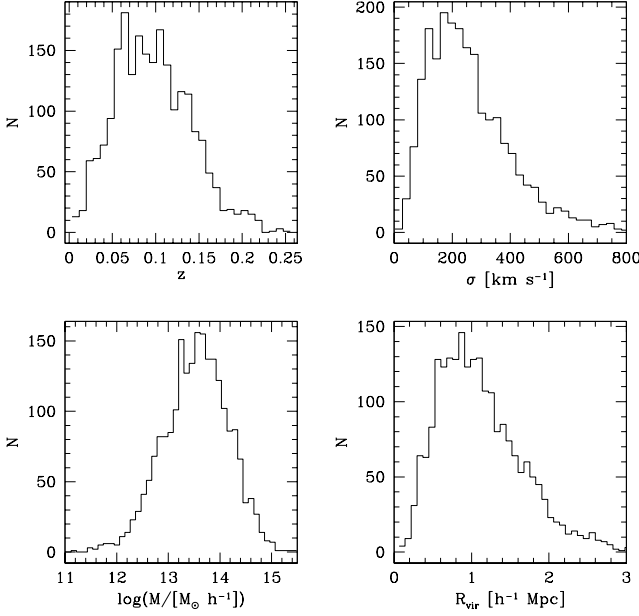


Figure 7. The upper-left panel shows the histogram describing the radial distribution for the groups identified in the 2dFGRS. The upper-right panel shows the distribution of groups velocity dispersions. The lower-left panel plots the virial mass distribution whereas the lower-right panel shows the distribution of groups virial radii.

Figure 5 shows the cone diagrams for galaxies (points) and groups (open circles) in the 2dF survey.

Estimation of the virial mass for galaxy groups is carried out using the following equation

$$M_{vir} = \frac{\sigma^2 R_V}{G} \quad (9)$$

where R_V is the virial radius of the system and σ is the velocity dispersion of member galaxies (Limber & Mathews 1960). The virial radius is estimated as

$$R_V = \frac{\pi}{2} R_{PV} \quad (10)$$

$$R_{PV} = \frac{N_g(N_g - 1)}{\sum_{i>j} R_{ij}^{-1}} \quad (11)$$

where R_{PV} is the projected virial radius, N_g is the number of galaxies members and R_{ij} the galaxy projected distances. The velocity dispersion σ is estimated using their observational counterpart, the line-of-sight velocity dispersion σ_v , $\sigma = \sqrt{3}\sigma_v$. In particular we use the methods described by Beers, Flynn & Gebhardt (1990) to obtain a robust estimation of the radial velocity dispersion. We apply the biweight estimator for groups with richness $N_{tot} \geq 15$ and the gapper estimator for poorer groups (Girardi et al. 1993, Girardi & Giuricin 2000). Despite these methods improve the velocity dispersion estimation in terms of efficiency and stability when dealing with small groups, it should be taken into account that small errors in the estimate of the velocity dispersion results in correspondingly larger errors in the derived mass.

The group properties estimation could be biased by the geometrical and sampling effects in the 2dF catalog. To deal

Table 2. Mean parameters of the 2dFGGC

N	$V_r (km/s)$	$\bar{\sigma} (km/s)$	$\bar{M} (h^{-1} M_\odot)$	$R_V (h^{-1} Mpc)$
2209	31500	261	8.5×10^{13}	1.12

with border effects we create a simple magnitude limited mock catalogue where limits in declination and right ascension exceed the corresponding to the 2dF catalog. Consequently we identify groups in this mock catalogue keeping those inside the 2dF border and we confront them with groups identified in a mock catalogue which emulate the 2dF geometry. As result, we observe no differences between the distribution of physical properties (R_V, σ and M) of these samples, showing that the complex geometry of the 2dF border do not affect group properties.

Another source of bias could be the variation of redshift completeness across the sky producing a wrong estimation of the physical properties in low completeness regions. In order to quantify this possible bias, we compare the physical properties of both, $c-m$ and m mock catalogues described in section 4, splitting these samples in high and low redshift completeness. In Figure 6 we show the histogram of R_V, σ and M for low (< 0.6 , upper panels) and high (≥ 0.6 , lower panels) completeness. Dotted lines correspond to m mock catalogue whereas the solid lines correspond to $c-m$ one. As it can be seen, only the virial radius in the low redshift completeness regions show some differences, nevertheless they do not produce any significant effect in the mass estimation.

Finally the distribution of the estimated physical properties are shown in Figure 7. In the upper-left panel we plot the redshift distribution with a mean redshift of $z \sim 0.1$, the lower-left panel shows the virial mass distribution, the upper-right panel correspond to the velocity dispersion distribution, and the virial radii distribution is shown in the remainder plot. The mean values of the 2dFGGC are quoted in Table 1.

6 CONCLUSIONS

In this paper we present a new catalogue of galaxy groups derived from the 2dFGRS, the largest sample of galaxies with spectroscopic redshifts at the present. The construction of this catalogue of groups (2dFGGC) was carried out introducing some modifications in the friend of friends algorithm developed by Huchra & Geller (1982) in order to take into account the different sky coverage variations in the sample. We have tested these modifications taking advantage of mock catalogues which allow us to explore the space parameter looking for the best values to maximize the group identification accuracy in redshift space. With these parameters ($\delta\rho/\rho = 80$ and $V_0 = 200 km sec^{-1}$) we obtain that $\sim 90\%$ of groups in real space match some group with at least four members in redshift space. Furthermore, the $\sim 30\%$ of groups in redshift space are spurious (no matched groups $\sim 6\%$ and groups associated with a binary or triplet $\sim 24\%$). We also find that the introduced modifications are able to detect $\sim 14\%$ more groups than the obtained by the original Huchra & Geller algorithm. Additionally, we explore the border effect and a possible bias due to redshift

completeness on the physical properties, finding that none of them produce significant effects on the final estimations.

Using the optimal identification parameters, the final group sample for the 2dF survey comprise 2209 groups of galaxies with mean redshift of $\bar{z} \sim 0.1$ and a mean velocity dispersion of $\bar{\sigma} = 261$ km/s. From the estimation of the virial masses for the galaxy groups we obtain a mean mass $\bar{M} = 8.5 \times 10^{13} h^{-1} M_{\odot}$ with a mean virial radius $\bar{R}_V = 1.12 h^{-1} Mpc$.

The new galaxy group catalogue is one of the largest groups samples until the present. For this reasons the new sample is more suitable for statistical studies than has been previously available.

ACKNOWLEDGMENTS

We want warmly thank to Carlton Baugh for reading the manuscript and helpful suggestions. We also thank to Peder Norberg and Shaun Cole for kindly providing the software describing the mask of the 2dFGRS and to the 2dFGRS Team for having made available the actual data sets of the sample. This work has been partially supported by Consejo de Investigaciones Científicas y Técnicas de la República Argentina (CONICET), the Secretaría de Ciencia y Técnica de la Universidad Nacional de Córdoba (SeCyT), the Consejo de Investigaciones Científicas y Tecnológicas de la Provincia de Córdoba (CONICOR) and Fundación Antorchas, Argentina.

REFERENCES

- Beers T. C., Flynn K., Gebhardt K., 1990, AJ, 100, 32.
 Colless M., et al. (2dFGRS Team), 2001, MNRAS, 328, 1039.
 Couchman H. M. P., Thomas P. A., Pearce F. R., 1995, ApJ 452, 797.
 da Costa L.N., Willmer C.N.A., Pellegrini P.S., Chaves O.L., Rite C., Maia M.A.G., Geller M.J., Latham D.W., Kurtz M.J., Huchra J.P., Ramella M., Fairall A.P., Smith C., Lipari S., 1998, AJ, 116, 1.
 De Propriis R., et al. (2dFGRS Team), 2002, MNRAS, 329, 87.
 Falco E.E., Kurtz M.J., Geller M.J., Huchra J.P., Peters J., Berlind P., Mink D.G., Tokarz S.P., Elwell B.G., 1999, PASP, 111, 438.
 Frederic J. J., 1995, ApJS, 97, 259.
 Girardi M., Biviano A., Giuricin G., Mardirossian F. & Mezzetti M., 1993, ApJ, 404, 38.
 Girardi M., Giuricin G., 2000, ApJ, 540, 45.
 Giuricin G., Marinoni C., Ceriani L., Pisani A., 2000, ApJ, 543, 178.
 Huchra J.P., Geller M.J., 1982, ApJ, 257, 423.
 Limber D.N., Mathews W.G., 1960, ApJ, 132, 286.
 Maddox S.J., Efstathiou G., Sutherland W.J., Loveday J., 1990a, MNRAS, 242, 43P.
 Maddox S.J., Efstathiou G., Sutherland W.J., Loveday J., 1990b, MNRAS, 243, 692.
 Maddox S.J., Efstathiou G., Sutherland W.J., 1996, MNRAS, 283, 1227.
 Merchán M.E., Maia M.A.G., Lambas D.G., 2000, ApJ, 545, 26.
 Nolthenius R., White S.D.M., 1987, MNRAS, 225, 505.
 Norberg P., et al. (2dFGRS Team), 2001a, MNRAS, 328, 64.
 Norberg P., et al. (2dFGRS Team), 2001b, submitted to MNRAS, astro-ph/0111011.
 Percival W.J., et al. (2dFGRS Team), 2001, MNRAS, 327, 1297.
 Ramella M., Geller M.J., Huchra J.P., 1990, ApJ, 353, 51.
 Ramella M., Pisani A., Geller M.J., 1997, ApJ, 113-2, 483.
 Ramella M., Geller M.J., Pisani A., da Costa L.N., 2002, AJ, in press.
 Tucker D.L., Oemler A.Jr., Hashimoto Y., Sheckman S.A., Kirshner R.P., Lin H., Landy S.D., Schechter P.L., Allam S.S., 2000, ApJS, 130, 237.